Focal Depths of Moderate and Large Size Earthquakes in Iran

A. Maggi[1], K. Priestley[2], and J. Jackson[2]

1. Ph.D. Student, Bullard Laboratories, Cambridge University, Madingley Road, Cambridge CB3 0EZ, UK, email: maggi@madingley.org
2. Faculty Members of the University, Bullard Laboratories, Cambridge University, Madingley Road, Cambridge CB3 0EZ, UK

ABSTRACT: *Accurate focal depth estimates are essential for the correct interpretation of seismicity data in terms of regional tectonics and earthquake hazard assessment. Published global earthquake catalogues are a common source of focal depth information, but how accurate are they? We compare estimates of focal depths from the Harvard CMT catalogue and the Engdahl et al [8] relocations of the ISC catalogue with those determined by teleseismic waveform inversion methods, and find that the catalogues can be in error by up to 60km.*

Keywords: Focal depths; Earthquakes; Iran; Seismicity; Waveform inversion

1. Introduction

Accurate focal depths for earthquakes are important in understanding the tectonics of a region and for evaluating earthquake hazards. For example the question of whether active subduction is still occurring beneath the Zagros critically depends on whether sub-crustal earthquakes occur there. Furthermore, estimates of peak ground motion from and earthquake depend critically on the focal depth. The most accurate method for determining the depth distribution of seismicity in a region is to monitor the moveout of local arrivals on closely spaced seismograph arrays. For most regions, however, the seismograph coverage is not dense enough for this method to be routinely employed, and we have to rely on less accurate methods.

The International Seismic Centre (*ISC*) and the National Earthquake Information Center (*NEIC*) routinely produce bulletins of earthquake hypocenter locations calculated from global teleseismic arrival times. These bulletins suffer notoriously from a trade-off between origin time and depth, which can cause errors in focal depth of several tens of *km* [9] in areas with high seismicity, but not very dense seismograph coverage. The accuracy of teleseismic hypocentral locations can be significantly improved by increasing the range of ray parameters used in the location procedure. Engdahl et al [8] have relocated all the earthquakes larger than *M* 5.2 in the *ISC* catalogue from 1964 to 1995 (subsequently updated to 1998) using an improved Earth model and many additional phases, particularly the teleseismic depth phases *pP*, *pwP*, and *sP*. These relocations, which we shall refer to as the *EHB* locations, are in general a significant improvement on the *ISC* locations. This is particularly apparent for subduction zones, where the *EHB* hypocenters give a much sharper image of the descending slabs.

Focal depth estimation is also routinely performed using long-period waveform data. Harvard publish centriod moment tensor (*CMT*) solutions determined from low-pass-filtered body and surface waves [6]. If the inversion is not sensitive to focal depth, the hypocenter is fixed to be consistent with waveform matching of reconstructed broad-band body waves [7]. The United States Geological Survey (*USGS*) perform moment tensor inversions on long-period vertical-component *P* waveforms obtained from digital recording stations [16, 17, 18], but these inversions cannot clearly resolve the focal depths of crustal earthquakes.

The focal depths of individual earthquakes of particular interest have also been determined by

detailed analysis of teleseismic waveforms. This type of study, which involves the generation of teleseismic synthetic seismograms, provides more accurate estimates of focal depth ($\pm 4km$) than the other teleseismic methods described above. In this paper, we compare the results obtained by waveform modelling with depths published in the *CMT* and *EHB* catalogues, for earthquakes in Iran and the surrounding region. These results are important for both tectonic interpretation and earthquake hazard assessment.

2. Teleseismic P and SH Waveform Inversion

We use the *MT*5 version of the McCaffrey and Abers [12] algorithm, which inverts *P* and *SH* waveform data for an earthquake to obtain its strike, dip, rake, centriod depth, seismic moment and source time function. The method was designed to use records from the World Wide Standard Seismic Network (*WWSSN*) 15-100 long-period instruments, which have a bandwidth that is well suited for the resolution of source parameters for shallow, moderate-size events [13]. In modern applications of the technique, broad-band records from the stations of the Global Digital Seismographic Network (*GDSN*) are used instead.

The earthquake source is constrained to be a double couple, or more than one if a multiple-rupture event is required to fit the data. Each source is represented as a point in space (the centriod); the time history of rupture is represented by a source time function constructed from a series of overlapping isosceles triangles. Synthetic seismograms are formed by combining direct *P* and *SH* waves with the surface reflections *pP*, *sP*, and *sS*. Amplitudes are corrected for geometrical spreading, and for an elastic attenuation using a Futterman *Q* operator with a value of t^* of 1 *s* for *P* and 4 *s* for *SH* waves. The synthetic seismograms include no arrivals due to upper mantle tripartitions or core phases, so this technique is only applicable to *P* waveforms recorded between 30^O and 90^O away, or to *SH* waves recorded between 30^O and 75^O away, for which the turning point of the waves is in the relatively uniform lower mantle.

The inversion procedure adjusts the relative amplitudes of the source time function elements, the centriod depth, the seismic moment and the focal mechanism (strike, dip, rake) to minimize the misfit between observed and synthetic seismograms. Focal depth and source time function influence the width of the first pulse, and the presence or absence of later pulses; the focal mechanism influences the polarity and relative amplitudes of pulses. The covariance matrix associated with the minimum misfit solution usually underestimates the true uncertainties associated with the source parameters. A better estimate of the uncertainties is obtained by fixing some of the source parameters at values close to those of the minimum misfit solution, inverting for the other parameters and seeing whether the match of synthetic to observed seismograms deteriorates [14, 19].

2.1. 31 July, 1994-Zagros

As an example of this method, we present the solution of an event in the Zagros mountains which was found to be shallow (14*km*) by Maggi et al [11] using teleseismic waveform inversion, despite being reported at much deeper depths by the Harvard *CMT* (49*km*), Engdahl (41*km*), *ISC* (*P-pP*: 44*km*), and *NEIC* (43*km*) catalogues. Figure (1) shows that the predicted *pP* arrival times for these catalogue depths are inconsistent with observed broad-band seismograms. The *P* and *SH* waveforms used in the full inversion for this event are shown in Figure (2), along with the best-fit synthetic waveforms. Although available stations are restricted to the northern half of the focal sphere, they are well distributed in azimuth, and the *P* and *SH* waveforms tightly constrain the focal mechanism. The minimum misfit solution is a thrust fault at a depth of 14*km*, with a simple time function about 2*s* long. The low dip (17^o) of the nodal plane is unusual in the Zagros, where high-angle (40^o-60^o) reverse faults are prevalent, but this mechanism is similar to the mechanisms of two other nearby events (1997-04-26 and 1980-10-19), listed in Table (1).

We assess the accuracy of the focal depth in Figure (3). The first line contains the minimum-misfit solution from Figure (2). In the second the depth was held fixed at 41*km* (as reported by the *EHB* catalogue) while all other source parameters were allowed to change. The result is a minimum in strike, dip, rake, source time function and moment space, but is very much a worse fit than the minimum misfit solution shown in the first line. In particular, there is no evidence in the *P* waveforms for the separation of the direct *P* and surface reflections, which would certainly be apparent if the depth were really 41*km*. The third and fourth lines show inversions in which the depth was held fixed at 18

Table 1. Iranian events: 1962-2000. Depths are measured in km; focal mechanisms are given as strike/dip/rake triplets, measured in degrees. In the CMT and EHB columns, indicates depths that have been fixed prior to relocation. An 'm' in the column indicates a multiple rupture earthquake.

Date	Time	Lat	Lon	M_w	P/SH	CMT	EHB	Mechanism	Reference
1962-09-01	19:20	35.70	49.80	6.98	10	-	-	101/52/70	Priestley et al (1994)
1968-06-23	09:16	29.66	51.20	5.49	9	-	32	136/45/88	Baker et al (1993)
1968-08-31	10:47	34.11	58.97	7.10	9	-	12	255/76/3	Baker (1993)
1968-09-01	07:27	34.10	58.25	6.25	9	-	8	115/54/85	Baker (1993)
1968-09-04	23:24	34.08	58.31	5.48	9	-	9	148/56/81	Baker (1993)
1968-09-11	19:17	34.02	59.54	5.56	6	-	3	78/90/16	Baker (1993)
1968-11-15	06:25	37.83	59.15	5.34	18	-	8	276/69/98	Baker (1993)
1969-01-03	03:16	37.11	57.81	5.45	7	-	8	132/50/95	Priestley et al (1994)
1970-07-30	00:52	37.85	55.92	6.35	11	-	9	293/56/-150	Priestley et al (1994)
1970-11-09	17:41	29.47	56.77	5.29	100	-	98	68/19/-124	Baker (1993)
1970-02-14	16:27	36.64	55.72	5.67	11	-	14	336/39/93	Priestley et al (1994)
1971-04-06	06:49	29.75	51.90	5.17	6	-	5	62/79/2	Baker et al (1993)
1971-05-26	02:41	35.56	58.23	5.58	13	-	16	89/26/32	Baker (1993)
1972-04-10	02:06	28.39	52.47	6.66m	9	-	5	288/49/99	Baker et al (1993)
1972-12-01	11:39	35.45	57.92	5.38	8	-	20	65/87/-25	Baker (1993)
1974-12-02	09:05	28.01	55.52	5.23	7	-	49	65/65/80	Baker (1993)
1976-04-22	17:03	28.61	52.09	5.65	7	-	23	312/52/80	Baker et al (1993)
1976-11-07	04:00	33.85	59.21	6.03m	8	-	6	84/79/12	Baker (1993)
1977-03-22	11:57	27.58	56.47	6.05	12	39	15	77/34/122	Maggi et al (2000)
1977-04-06	13:36	31.87	50.69	5.86	6	41	10	112/64/132	Baker (1993)
1977-12-10	05:46	27.68	56.60	5.57	18	47	13	291/28/138	Maggi et al (2000)
1977-12-19	23:34	30.89	56.45	5.81	7	31	13	58/82/36	Baker (1993)
1978-11-04	15:22	37.71	48.97	6.12	21	34	26	346/79/95	Priestley et al (1994)
1979-01-16	09:50	33.96	59.51	6.48m	11	33†	8	162/66/115	Baker (1993)
1979-02-13	10:36	33.34	57.44	5.58	11	33†	15	332/27/120	Baker (1993)
1979-11-14	02:21	34.04	59.80	6.57m	10	33†	8	160/89/-177	Baker (1993)
1979-11-27	17:10	34.08	59.79	7.09m	8	10	6	80/89/-11	Baker (1993)
1979-12-07	09:24	34.10	59.91	5.93	10	31	13	20/69/173	Baker (1993)
1979-12-09	09:12	35.15	56.87	5.55	9	48	15	352/36/99	Baker (1993)
1980-01-12	15:31	33.55	57.26	6.02	13	33	10	120/77/75	Baker (1993)
1980-05-04	18:35	38.07	49.04	6.34	15	46	28	181/84/-93	Priestley et al (1994)
1980-10-19	17:24	32.70	48.59	5.60	17	42	17	327/19/120	Maggi et al (2000)
1980-12-19	01:16	34.47	50.64	6.03	14	33†	12	115/41/120	Priestley et al (1994)
1980-12-22	12:51	34.41	50.63	5.56	15	41	18	113/56/125	Priestley et al (1994)

Table 1. Continued ... Iranian events

Date	Time	Lat	Lon	M_w	P/SH	CMT	EHB	Mechanism	Reference
1981-06-11	07:24	29.83	57.70	6.58m	20	33†	15	169/52/156	Berberian et al (2001)
1981-07-28	17:22	29.93	57.78	7.05m	14	33†	13	185/42/140	Baker (1993)
1981-08-04	18:35	38.20	49.43	5.52	20	25	29	154/35/32	Priestley et al (1994)
1983-07-12	11:34	27.61	56.41	5.93	17	33†	20	227/50/75	Maggi et al (2000)
1983-07-22	02:41	36.93	49.24	5.45	10	-	27	120/35/83	Priestley et al (1994)
1984-02-22	05:44	39.89	54.11	5.74	27	33	3	106/60/174	Priestley et al (1994)
1984-08-06	11:14	30.78	57.18	5.29	11	33†	3	94/35/86	Baker (1993)
1985-02-02	20:52	28.34	52.97	5.56m	11	33†	15	128/37/91	Baker (1993)
1985-08-07	15:43	27.77	53.02	5.36	17	15	11	290/56/88	Baker (1993)
1985-08-16	10:46	37.20	59.44	5.49	9	33†	9	256/80/56	Baker (1993)
1985-10-29	14:23	36.79	54.84	6.16	13	33†	50	246/66/71	Priestley et al (1994)
1986-03-06	00:05	40.38	51.62	6.38m	31	33	22	299/88/-85	Priestley et al (1994)
1986-07-12	07:54	29.88	51.55	5.54	4	33†	6	4/73/-159	Baker et al (1993)
1986-12-20	23:47	29.88	51.56	5.29	8	33†	12	344/65/163	Baker et al (1993)
1987-04-29	01:45	27.42	56.11	5.65	10	34	8	265/41/112	Maggi et al (2000)
1987-08-10	10:52	29.88	63.88	5.93	155	157	163	346/31/-50	Maggi et al (2000)
1987-09-07	11:32	39.47	54.81	5.51	30	38	35	305/10/103	Priestley et al (1994)
1987-12-18	16:24	28.11	56.63	5.77	10	35	21	160/44/-145	Baker (1993)
1988-08-11	16:00	29.93	51.56	5.52	7	31	15	3/69/-175	Baker et al (1993)
1988-08-11	16:04	29.89	51.64	5.81	9	33†	15	350/82/-166	Baker et al (1993)
1988-12-06	13:20	29.87	51.61	5.60	10	37	12	357/74/-162	Baker et al (1993)
1989-09-16	02:05	40.35	51.57	6.49	31	33	45	80/26/-135	Priestley et al (1994)
1989-09-17	00:53	40.23	51.81	6.16	35	33	49	277/50/-111	Priestley et al (1994)
1989-11-20	04:19	29.85	57.71	5.83	10	33†	18	145/69/-172	Berberian et al (2001)
1990-06-21	09:02	36.61	49.81	5.59	10	10	13	0/62/95	Jackson et al (2002)
1990-09-26	15:32	29.03	60.89	5.51	8	33†	5	15/76/166	Baker et al (1993)
1990-11-06	18:45	28.21	55.45	6.50	7	25	10	275/30/101	Maggi et al (2000)
1991-11-28	17:20	36.84	49.61	5.56	11	14	43	356/51/81	Jackson et al (2002)
1993-06-22	16:32	30.15	50.81	5.24	5	33†	42	301/44/13	Maggi et al (2000)
1993-08-31	06:55	41.87	49.47	5.19	75	83	89	237/36/63	Jackson et al (2002)
1994-02-23	08:02	30.80	60.57	6.11	7	10	11	143/29/96	Berberian et al (2000)
1994-02-24	00:11	30.82	60.53	6.24	9	13	10	160/47/111	Jackson et al (2002)
1994-02-26	02:31	30.78	60.55	6.01	6	12	7	154/36/110	Jackson et al (2002)
1994-02-28	11:13	30.82	60.55	5.54	6	10	67	140/33/91	Jackson et al (2002)

Table 1. Continued ... Iranian events

Date	Time	Lat	Lon	M_w	P/SH	CMT	EHB	Mechanism	Reference
1994-06-20	09:09	29.06	52.67	5.79	9	17	14	255/74/-3	Maggi et al (2000)
1994-07-01	10:12	40.19	53.35	5.59	41	44	45	90/71/96	Jackson et al (2002)
1994-07-01	19:50	40.20	53.37	5.11	41	43	45	93/71/97	Jackson et al (2002)
1994-07-31	05:15	32.67	48.41	5.47	14	49	41	288/17/90	Maggi et al (2000)
1995-10-29	06:27	39.56	51.90	5.32	61	64	40	316/76/-13	Jackson et al (2002)
1997-02-04	09:53	37.39	57.33	5.39	13	10	11	333/63/154	Jackson et al (2002)
1997-02-04	10:37	37.39	57.35	6.57	6	10	18	59/73/25	Jackson et al (2002)
1997-02-28	12:57	38.10	47.79	6.00	9	10	38	273/89/-171	Jackson et al (2002)
1997-04-19	05:53	28.02	56.88	5.48	19	27	30	219/47/13	Maggi et al (2000)
1997-05-07	16:16	40.33	51.63	5.20	50	51	48	287/41/-115	Jackson et al (2002)
1997-05-10	07:57	33.86	59.83	7.12	13	10	11	156/89/-150	Berberian et al (1999)
1997-06-20	12:57	32.33	59.96	5.36	2	10	20	188/79/-178	Berberian et al (1999)
1997-06-25	19:38	33.94	59.48	5.73	8	10	15†	181/87/170	Berberian et al (1999)
1997-10-20	06:09	28.46	57.26	5.22	28	33	36	244/19/47	Maggi et al (2000)
1998-03-14	19:40	30.08	57.61	6.57	5	9	5	156/54/-165	Jackson et al (2002)
1998-06-10	08:30	28.22	58.49	5.25	85	88	88	117/7/-28	Maggi et al (2000)
1998-07-09	14:19	38.71	48.50	5.69	27	26	28	342/89/98	Jackson et al (2002)
1999-05-06	23:00	29.54	51.93	6.12	7	33†	-	44/82/-6	Maggi et al (2000)
2000-08-22	16:55	38.07	57.19	5.59	4	10	-	133/69/171	Jackson et al (2002)

(M_ω

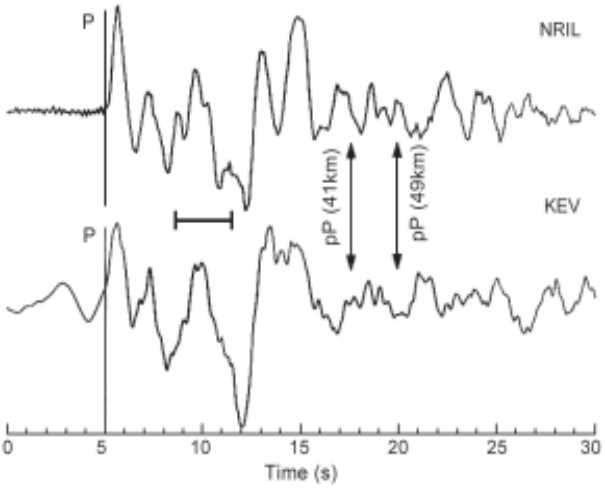

Figure 1. Broad-band records for the stations NRIL (distance 4801km, azimuth 19°) and KEV (distance 4346km, azimuth 348°). The predicted pP times for depths of 41km (EHB) and 49km (CMT) are shown by arrows, and do not match the seismograms. The horizontal bar shows the predicted arrival of the surface reflections for a depth of 15km.

and 10*km*, while all other source parameters were free. At 18*km* (line 3) the first at *LVZ* (*P*), *TATO* (*SH*) and *PAB* (*SH*) are significantly worse than in line 1. The fits in line 4 (depth 10*km*) are not significantly worse than in line 1, but the inversion has compensated for the shallow depth by source time function to have a double pulse, which is unlikely for an event of this size 5.5). If the time function is forced to be short, with the depth fixed at 10*km*, the fit at all stations deteriorates (line 5). We conclude that the uncertainty in the estimate of the centriod depth for this earthquake (14*km*) is no greater than $\pm$ 4*km*, and that this earthquake is significantly shallower than reported in any of the earthquake catalogues.

3. Focal Depths in Iran

The waveform inversion method described in this paper has been applied to 87 moderate to large size

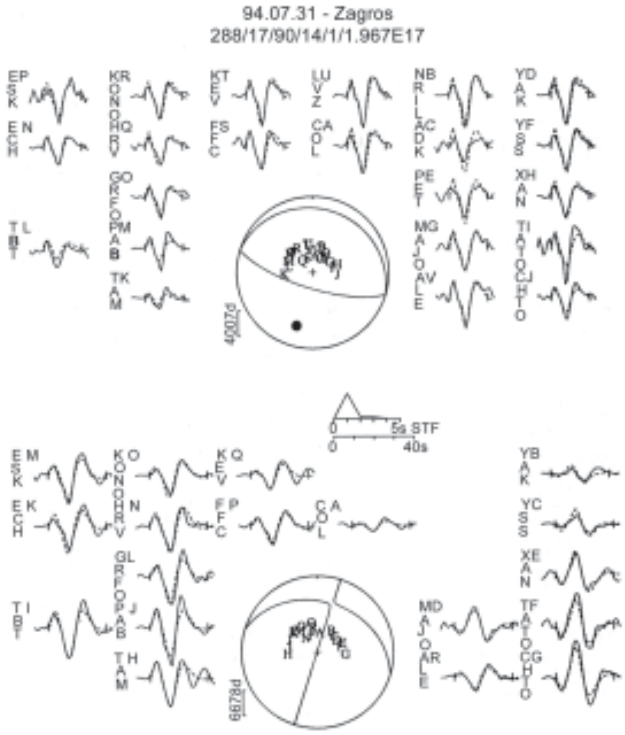

Figure 2. Minimum misfit solution for the event of 31 July 1994 in the Zagros. The values beneath the event header give strike, dip, rake, depth in km and seismic moment (in units of Nm). This solution was calculated using velocity model consisting of a 10km thick layer with V_P = 6.0k, s^{-1}, V_S = 3.45 kms^{-1}, = 2.78g cc^{-1} over a half space with V_P-6.8km s^{-1}, VS-3.92km s^{-1} and = 2.91g cc^{-1}. The upper sphere shows the P wave radiation pattern and the lower sphere the SH radiation pattern. Both are lower-hemisphere projections. The station code by each waveform is accompanied by a letter corresponding to its position in the focal sphere. The positions are ordered clockwise by azimuth. The solid lines are the observed waveforms, the dashed lines are the synthetic waveforms. The inversion window is marked by sold bars at either end of the waveform. P and T axes are represented by solid and open circles respectively on the P-wave radiation pattern. The source time function is shown below the P focal sphere, with the waveform time scale below it. This figure was modified from Maggi et al [11] Figure (2).

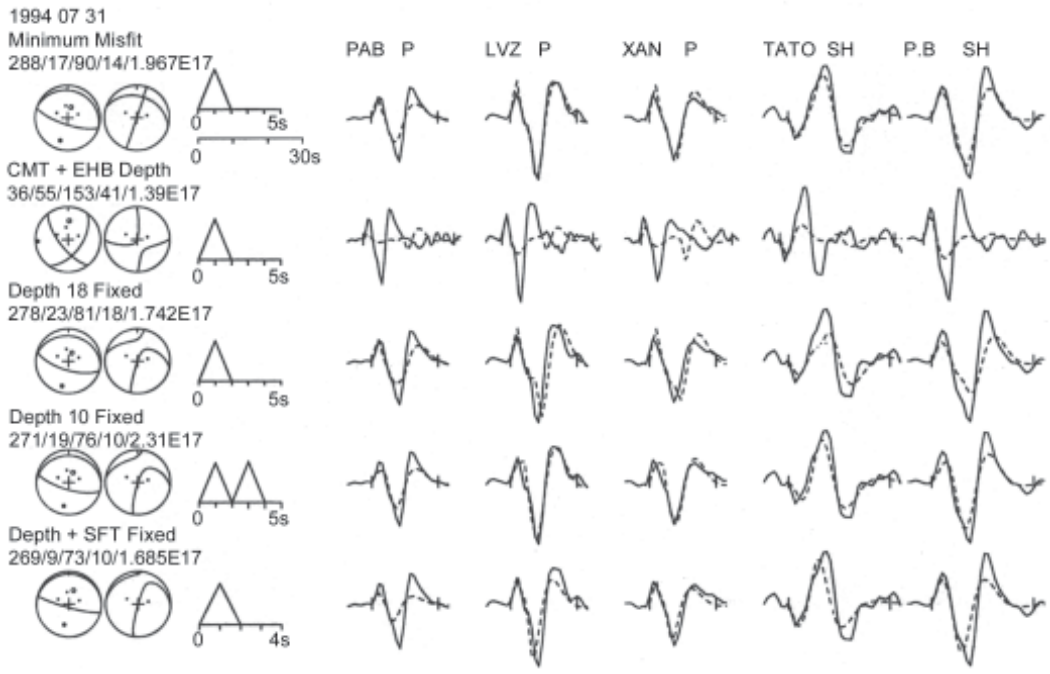

Figure 3. Comparisons between different inversion solutions for the 1994 July 31 Zagros earthquake. The P and SH radiation patterns are shown in first column, with the strike, dip, rake , depth in km and scalar moment in Nm above the two focal spheres. The source time function for each solution is in the second column, followed by the observed (solid) and synthetic (dashed) waveforms. Line 1: the minimum misfit solution; line 2: the result of an inversion started from the published Harvard CMT solution with the fixed EHB depth of 41 km; lines 3-5: Tests for the uncertainty in the depth; in all these inversions the depth was held fixed and all other parameters were free to change. In line 5 the duration of the source time function was also held fixed.

earthquakes that have occurred in Iran and the surrounding region. Table (1) lists their locations, depths, focal mechanisms, references to the waveform modelling studies, and the depths reported by the Harvard *CMT* and *EHB* catalogues. Comparison of the *P/SH*, *EHB* and *CMT* columns of Table (1) reveals that focal depths in earthquake catalogues can be significantly in error, sometimes by as much as 60*km*.

The discrepancy between catalogue and waveform-determined depths depends on both focal depth and magnitude, as illustrated by Figure (4). The dependence is stronger for the *EHB* (black) discrepancies, which decrease for gennuinely deeper events and larger magnitudes. This dependence is unsurprising. The *EHB* depth determinations are based on reported high-frequency regional and teleseismic *P*, *S*, and *PKP* phases, and the teleseismic depth phases *pP*, *pwP* and *sP*. At depths greater than ~50*km*, the *pP-P* time separation is greater than ~15*s*, the surface reflections are clear and easily recognized, and the source time function is simple and impulsive. At shallow depths, however, *pP* and *sP* can easily be misidentified and confused with other phases arising from near-source structure, complex source-time-functions or multiple ruptures. For small-magnitude events, waveforms at teleseismic distances have small signal-to-noise ratios, making the depth phases even harder to identify. The signal-to-noise ratio generally improves at regional distances, but here the complex structure though which the seismic waves propagate causes the seismograms themselves to be rather complex, leading again to difficulties in finding and identifying depth phases.

The discrepancies in focal depth between the *EHB* or *CMT* catalogues and waveform studies also depend on the location of the earthquakes, Figure (5): both catalogues show larger errors for earthquakes in the Zagros mountains and close to the Caspian Sea. This location dependence is due to the uneven distribution of seismograph stations at regional distances from these regions. The Engdahl et al [8] relocation procedure is particularly unreliable if there are no

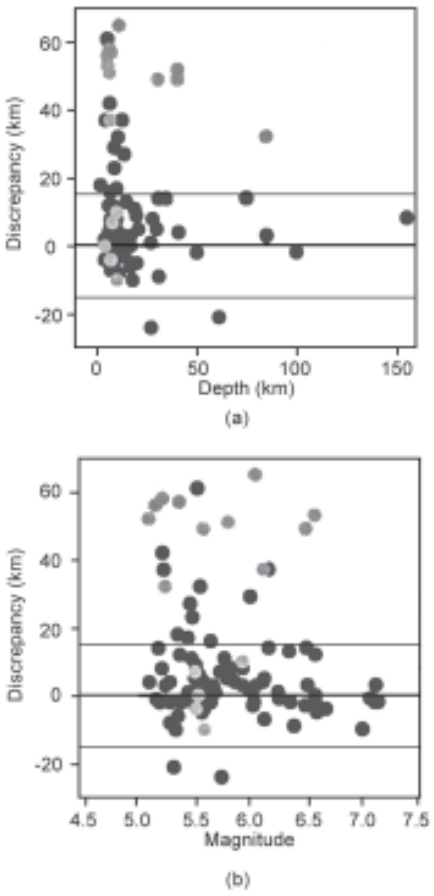

Figure 4. Depth and magnitude dependence of the focal depth discrepancy. Focal depth discrepancy (waveform depth-catalogue) is plotted against (a) waveform depth and (b) moment magnitude for the events in Table (1); EHB discrepancies are represented by black circles, and CMT discrepancies by gray circles. The thin lines lie at 15km, the official standard deviation of the EHB catalogue.

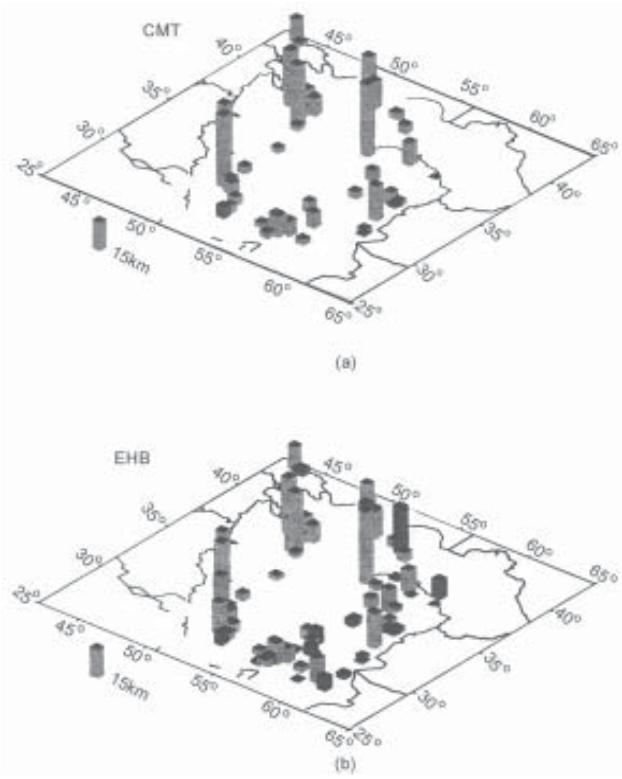

Figure 5. The discrepancy between (a) the Harvard CMT depths and (b) the EHB catalogue depths and the waveform determined depths for the earthquakes in Table (1). Light grey columns indicate that the catalogue depths are greater than the waveform determined depths, while dark grey column indicates they are shallower.

stations within the inflection point of the travel time curve: the identification of depth phases as *pP* as apposed to *sP* becomes dependent on the starting depth for the relocation [11].

3.1. Focal Depths Influence Tectonic Interpretation

Accurate focal depths are essential for a correct tectonic interpretation of seismic activity. Figure (6) shows how the picture of seismic activity changes with different focal depth datasets. If we use the results from the waveform inversion studies in Table (1) and separate the shallow (<33*km* depth) and deep (>33*km* depth) earthquakes, Figures (6a) and (6b), we see that most of the seismicity is shallow and occurs well within the continental crust; deep earthquakes are confined to zones where subduction of oceanic lithosphere is taking place. i.e. the Markran subduction zone in the south and the Apsheron-Balkhan sill, where the South Caspian Basin is subducting beneath the central Caspian [15, 10].

This simple picture changes substantially if we use focal depths from the Harvard *CMT* catalogue, Figures (6c) and (6d). There now seem to be a number of deep events both in the north, where they border the north and western sides of the South Caspian Basin, and in the southwest, where they continue westwards from the Makran subduction

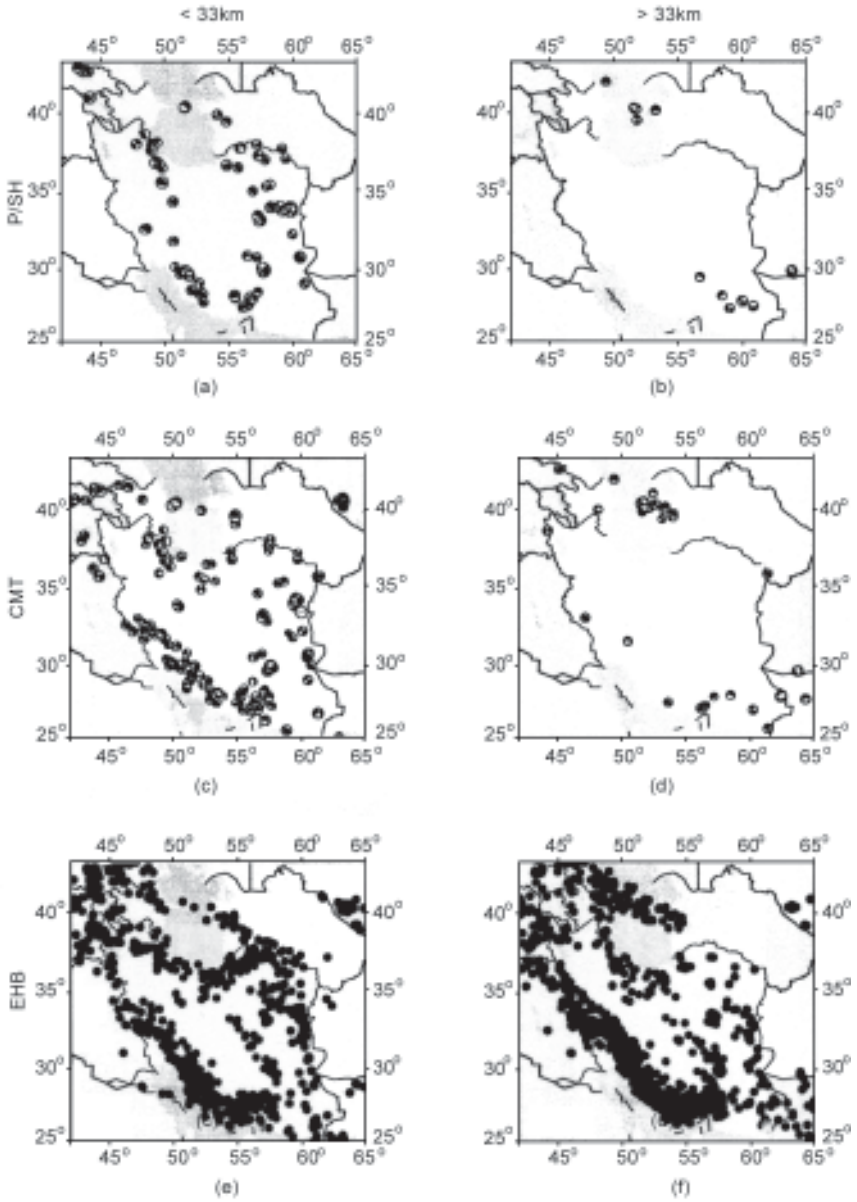

Figure 6. The spatial distribution of shallow (<33km) and deep (>33km) seismicity for (a-b) the events in Table (1), (c-d) events in the Harvard CMT catalogue and (e-f) events in the EHB catalogue. Events with depths of 33km (including those fixed at this depth by the Harvard CMT catalogue) have been classed as shallow. The low magnitude cutoff for all plots in M_w5.1, the magnitude of the smallest event for which waveform inversion was performed.

zone through the Zagros mountains up to about $35^{O}N$. The picture changes yet again when we plot the distributions of shallow and deep events from the *EHB* catalogue, Figures (6e) and (6f): it now seems that the majority of earthquakes in the region occur below 33*km* depth, in the continental mantle, the opposite conclusion to that made using waveform determined focal depths.

4. Conclusion

We have compared focal depth estimates from two published earthquake catalogues, the Harvard *CMT* catalogue and the Engdahl et al [8] relocations of the *ISC* catalogue, and find that:

- Focal depths published in earthquake catalogues are in error by up to 60*km* for events in Iran and the surrounding region.
- The errors are greatest for shallow, crustal earthquakes of moderate size 5.5).
- The errors are widespread enough to dramatically change the picture of seismicity in the region.

We therefore recommend that only focal depths determined using accurate methods, such as local network recordings or teleseismic waveform inversion, be used in studies of regional tectonics or seismic hazard assessment.

($M_{\omega} \sim$

References

1. Baker, C. (1993). "The Active Seismicity and Tectonics of Iran", Ph.D. Thesis, University of Cambridge, 228pp.

2. Baker, C., Jackson, J., and Priestley, K. (1993). "Earthquakes on the Kazerun Line in the Zagros Mountains of Iran: Strike-Slip Faulting within a Fold- and-Thrust Belt", *Geophys. J. Int.*, **115**, 41-61.

3. Berberian, M., Jackson, J.A., Fielding, E., Parsons, B.E., Priestley, K., Qorashi, M., Talebian, M., Walker, R., Wright, T.J., and Baker, C. (2001). "The 14 March, 1998 Fandoqa Earthquake (m_{ω} 6.6) in Kerman Province, Southeast Iran: Rupture of the 1981 Sirch Earthquake Fault, Triggering of Slip on Adjacent Thrusts, and the Active Tectonic of the Gowk Fault Zone", *Geophys. J. Int.*, **146**, 371-398.

4. Berberian, M., Jackson, J.A., Qorashi, M., Khatib, M.M., Priestley, K., Talebian, T., and Ghafory-Ashtiany, M. (1999). "The 1997 May 10 Zirkuh (Qa'enat) Earthquake (m_{ω} = 7.2): Faulting Along the Sistan Suture Zone of Eastern Iran", *Geophys. J. Int.*, **136**, 671-694.

5. Berberian, M., Jackson, J.A., Qorashi, M., Talebian, M., Khatib, M., and Priestley, K. (2000). "The 1994 Sefidabeh Earthquake in Eastern Iran: Blind Thrusting and Bedding-Plane Slip on a Growing Anticline, and Active Tectonics of the Sistan Suture Zone", *Geophys. J. Int.*, **142**, 283-299.

6. Dziewonski, A.M. Chou, T.A., and Woodhouse, J.H. (1981). "Determination of Earthquake Source Parameters from Waveform Data for Studies of Global and Regional Seismicity", *J. Geophys. Res.*, **86**, 2825-2852.

7. Ekstrom, G.A. (1989). "A Very Broad-Band Inversion Method for the Recovery of Earthquake Source Parameters", *Tectonophysics*, **166**, 73-100.

8. Engdahl, E.R., Van Der Hilst, R., and Bulland, R. (1998). "Global Teleseismic Earthquake Relocation with Improved Travel Times and Procedures for Depth Determination", *B. Seismol. Soc. Am.*, **88**, 722-743.

9. Jackson, J. (1980). "Errors in Focal Depth Determination and the Depth of Seismicity in Iran and Turkey", *Geophys. J. R. Astr. Soc.*, **61**, 285-301.

10. Jackson, J., Priestley, K., Allen, M., and Berberian, M. (2002). "Active Tectonics of the South Caspian Basin", *Geophys. J. Int.*, In Review.

11. Maggi, A., Jackson, J.A., Priestley, K., and Baker, C. (2000). "A Re-Assessment of Focal Depth Distribution in Southern Iran, The Tien Shan and Northern India: Do Earthquakes Really Occur in the Continental Mantle?", *Geophys. J. Int.*, **143**, 629-661.

12. McCaffrey, R. and Abers, J. (1988). "SYN3: A Program for Inversion of Teleseismic Body Wave form on Microcomputers", Technical Report AFGL-TR-0099, Air Force Geophysical Laboratory, Hanscomb Air Force Base, Massachusetts.

13. McCaffrey, R. and Nabelek, F. (1987). "Earthquakes, Gravity and the Origin of the Bali Basin: An Example of a Nascent Continental Fold-and-Thrust Belt", *J. Geophys. Res.*, **92**, 441-460.

14. Molnar, P. and Lyon-Caen, H. (1989). "Fault Plane Solutions of Earthquakes and Active Tectonics of the Tibetan Plateau and Its Margins", *Geophys. J. Int.*, **99**, 123-153.

15. Priestley, K., Baker, C., and Jackson, J. (1994). "Implications of Earthquake Focal Mechanism Data for the Active Tectonics of the South Caspian Basin and Surrounding Regions", *Geophys. J. Int.*, **118**, 111-141.

16. Sipkin, S.A. (1982). "Estimation of Earthquake Source Parameter by the Inversion of Waveform Data, Synthetic Seismograms", *Phys. Earth Planet. In.*, **30**, 242-259.

17. Sipkin, S.A. (1986a). "Estimation of Earthquake Source Parameters by the Inversion of Waveform Data: Global Seismicity 1981-1983", *B. Seismol. Soc. Am.*, **76**, 1515-1541.

18. Sipkin, S.A. (1986b). "Interpretation of Non-Double-Couple Earthquake Source Mechanisms Derived from Moment Tensor Inversion", *J. Geophys. Res.*, **91**, 531-547.

19. Taymaz, T., Jackson, J., and McKenzie, D. (1991). "Active Tectonics of the North and Central Aegean Sea", *Geophys. J. Int.*, **106**, 433-490.